Science of the Total Environment 642 (2018) 968–978

Contents lists available at ScienceDirect

Science of the Total Environment

journal homepage: www.elsevier.com/locate/scitotenv

Shifts of environmental and phytoplankton variables in a regulated river: A spatial-driven analysis

Laia Sabater-Liesa [a], Antoni Ginebreda [a,*], Damià Barceló [a,b]

[a] Department of Environmental Chemistry, IDAEA-CSIC, Jordi Girona 18-26, 08034 Barcelona, Spain
[b] ICRA, Carrer Emili Grahit 101, Girona 17003, Spain

HIGHLIGHTS

- Phytoplankton community structure and composition do not absorb reservoirs impact.
- Phytoplankton and environmental variables show spatial discontinuities and river fragmentation.
- There is a strong neighbor influence on the longitudinal river dynamics of environmental variables.
- An adaptive response of the phytoplankton taxa and rapid colonization of opportunist species after reservoirs is observed.

GRAPHICAL ABSTRACT

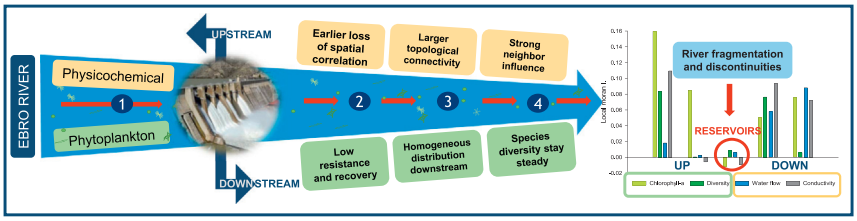

ARTICLE INFO

Article history:
Received 27 April 2018
Received in revised form 5 June 2018
Accepted 8 June 2018
Available online 19 June 2018

Keywords:
Phytoplankton
Environmental variables
Ebro River
Spatial autocorrelation
Longitudinal connectivity
Resistance and resilience

ABSTRACT

The longitudinal structure of the environmental and phytoplankton variables was investigated in the Ebro River (NE Spain), which is heavily affected by water abstraction and regulation. A first exploration indicated that the phytoplankton community did not resist the impact of reservoirs and barely recovered downstream of them. The spatial analysis showed that the responses of the phytoplankton and environmental variables were not uniform. The two set of variables revealed spatial variability discontinuities and river fragmentation upstream and downstream from the reservoirs. Reservoirs caused the replacement of spatially heterogeneous habitats by homogeneous spatially distributed water bodies, these new environmental conditions downstream benefiting the opportunist and cosmopolitan algal taxa. The application of a spatial auto-regression model to algal biomass (chlorophyll-*a*) permitted to capture the relevance and contribution of extra-local influences in the river ecosystem.

1. Introduction

River networks have an asymmetrical configuration which determines unidirectional physical and chemical processes (Frissell et al., 1986). The imposed downstream direction in environmental conditions greatly determines the biological structure of river (Vannote et al., 1980; Wehr and Descy, 1998), though geomorphological complexity configures non-linear connections (Delong and Thorp, 2006). So forth, neighboring sites are not independent one from the other, and this can be reflected both in the hydrological and environmental conditions as well as in the composition and relative abundance of biological assemblages (Amoros and Bornette, 2002; Tockner et al., 1999; Ward and Stanford, 1995). This complex pattern is further complicated when hydraulic infrastructures (dams, weirs, channels) occur in the river (Lobera et al., 2017). Largely regulated rivers show alterations of the water regime and its chemical quality, which affect biological assemblages (Dynesius and Nilsson, 1994; Nilsson et al., 2005). The

* Corresponding author.
E-mail address: antoni.ginebreda@cid.csic.es (A. Ginebreda).

https://doi.org/10.1016/j.scitotenv.2018.06.096

regulation capacity of reservoirs is one of the strongest causes for river discontinuity (Ward and Stanford, 1983), but their impact on environmental and biological variables is not necessarily analogous (Bunn and Arthington, 2002). It is unknown yet if the ability to resist regulation effects, and the ability to recover after them, is parallel between ones and the others.

One of the most sensitive elements in large river ecosystems is phytoplankton. The phytoplankton community plays a central role as primary producers in the functioning of large rivers (Dale, 2001; Wehr and Descy, 1998). River phytoplankton occurs as a balance result of the advective forces occurring in flowing waters and the in situ population growth rates (Reynolds, 2006). In this delicate balance, river phytoplankton is affected both by local environmental factors (light and nutrient availability, water temperature, grazing pressure) as well as by the upstream influence of continuous seeding and hydrological and chemical conditions. Here we use the phytoplankton community composition and its associated biomass (planktonic chlorophyll-*a*) as the biological receptors to be tested in the river because of regulation, and compare their changes in structure with those occurring in the environmental variables.

In that context, the Ebro River offers a suitable case study to explore the spatial structure of an ecosystem impacted by man-made perturbation. The Ebro River is one of the largest rivers in the Iberian Peninsula, strongly regulated by dams since the 1940s'. Around 190 dams are spread across the whole basin, impounding 57% of the mean annual runoff (Romaní et al., 2011). The location of the three large reservoirs (Mequinenza, Ribarroja and Flix) in the middle-lower section of the river causes a large disruption to the sites downstream. These reservoirs cause water thermal alteration downstream (Prats et al., 2010), contribute to retain sediments (Batalla and Vericat, 2011), and disrupt the biogeochemical nutrients cycles and the phytoplankton community structure (Sabater et al., 2008; Tornes et al., 2014). Since the basin is subjected to multiple human activities which produce impacts like inorganic and organic pollution and water abstraction (Batalla et al., 2004; Lacorte et al., 2006; Navarro-Ortega and Barceló, 2011), effects might be complex on both water quality and phytoplankton assemblages. The size and position of these reservoirs offer a good setting for the analysis of the phytoplankton and environmental variables responses to the impact, showing in which way their respective spatial patterns differ or resemble.

In order to do so, we apply an analogous approach to that used on trophic webs and metapopulations analysis, able to deal with complex systems in which different constituents ("nodes") interact ("links") to each other (Nordstrom and Bonsdorff, 2017; Wallach et al., 2017). We use this as starting point to capture the river topology and connections among neighboring nodes, where variables were measured (monitoring sites) and the anthropogenic effects on this arrangement were evaluated by using appropriate tools commonly used in the spatial analysis (Fischer and Wang, 2011; Ginebreda et al., 2018). Whereas either time or spatial data series could be in principle equally used in autocorrelation modeling of phytoplankton indicators, their performance depends on (a) the connectivity and heterogeneity of the area under study, (b) the spatial and temporal scales of the variable considered and (c) the easiness of monitoring. Spatial autocorrelation works better on heterogeneous environments, and its analysis takes into account the connectivity (Dakos et al., 2010). On the other hand, the timescales that govern phytoplankton succession (weeks) require of an extensive monitoring effort far beyond the one required for a spatial study. Based on that, the spatial analysis approach is a convenient alternative to time series when available data are not sufficiently complete. In this paper we implement a method to analyze and compare the spatial patterns of environmental and biological variables in rivers systems submitted to regulation. The identification of 'stability' properties (resistance and resilience), and thus, the interpretation in terms of connectivity and longitudinal patterns are aimed to test the hypothesis that regulation produces uncoupled responses on the environmental and phytoplankton variables, further compromising the ability of phytoplankton community to resist and recover. While the longitudinal dynamics of environmental variables supposedly has a strong neighbor influence, the response of phytoplankton is likely more complex as a result of conjoint local and extra-local influences. The spatial dimension may then provide understanding on how the different elements of river ecosystem respond to regulation.

2. Material and methods

2.1. Study area

The Ebro basin is located in the Northeastern part of the Iberian Peninsula occupying a total surface of 85,362 km^2. The main river is 910 km length and flows from the Cantabrian mountains to the Mediterranean sea (Romaní et al., 2011). In the Ebro mainstream there is a system of three consecutive large reservoirs, Mequinenza (1500×10^6 m^3), Riba-roja (210×10^6 m^3) and Flix (11×10^6 m^3) that regulate the hydrology of the lower part (Prats et al., 2010). These reservoirs cause major changes in the hydromorphological dynamics by altering floods peaks (López-Moreno et al., 2002) as well as by retaining sediments (Buendia et al., 2016).

2.2. Data collection

For this study we used data from several published studies (Artigas et al., 2012; Sabater et al., 2008; Tornes et al., 2014), as well as public data from the Confederación Hidrográfica del Ebro webpage (http://www.chebro.es). Using these sources, we selected data from twelve sites located in the mid-lower course from Zaragoza to the proximity of the river mouth (Fig. 1). Six of the sites (Zaragoza, EB01; Pina Ebro, EB02; Quinto, EB03; Zaida, EB04; Sástago, EB05; Escatrón, EB06) were located upstream of the Mequinenza, Riba-roja and Flix reservoirs. One site (Almatret, EB07) was placed between the first two dams, and the remaining five (Flix, EB08; Ascó, EB09; Móra d'Ebre, EB10; Benifallet, EB11; Xerta, EB12) were located downstream to the reservoirs.

We collected some data on abiotic and biotic variables to characterize the ecosystem response to regulation. Regarding biological variables, we used metrics on the phytoplankton biomass (biovolume and chlorophyll-*a* concentration) and community structure (Shannon-Wiener diversity, cell density). Both biovolume and chlorophyll-*a* concentration have been used as surrogate of biomass (Hillebrand et al., 1999); while the Shannon diversity index (H′) characterizes the taxonomic diversity in a community. The selected physical and chemical variables included water temperature, conductivity, water flow and nutrients. NH_4^+ and NO_3^- were considered together as dissolved inorganic nitrogen (DIN), comparable to, soluble reactive phosphorus (SRP), Dissolved Inorganic Carbon (DIC), Dissolved Organic Carbon (DOC) and Dissolved Organic Nitrogen (DON).

Phytoplankton and environmental data covered eighteen sampling campaigns between 2008 and 2013. The dataset included samples from different hydrological conditions, low waters and high water periods, occurring in the river (Artigas et al., 2012). Therefore, the data we used accounted for 350 km of the main river axis over 5 years (Table S1a and b).

2.3. Data analysis

The sequence of analysis is summarized in Fig. 2. Briefly, the stress effect of reservoirs into phytoplankton was analyzed by means of two stability properties, i.e., resilience and resistance (Grimm and Wissel, 1997). These are dynamic properties largely dependent on the connections of the ecosystem (Pimm, 1984); resilience is the capacity of the system to return to a reference state after a disturbance, while resistance refers to staying essentially unchanged despite the perturbation

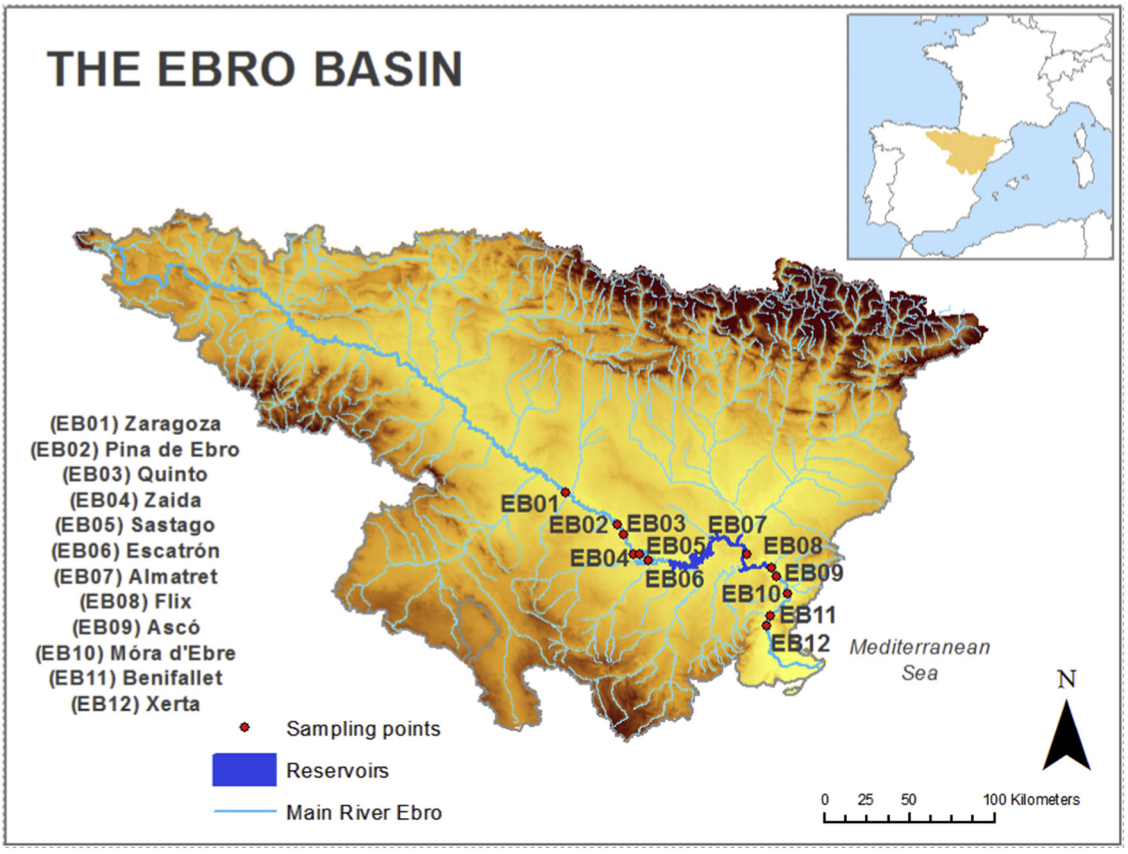

Fig. 1. The Ebro river basin. The reservoirs are highlighted and the sampling points are numbered.

(Holling, 1973). To that end, appropriate indexes quantifying these properties are proposed.

In a second phase of the analysis, we examined the spatial distribution of the biological and environmental variables, separating the variability in the river sections upstream and downstream the reservoirs. We further explored the spatial connectivity of these variables using spatial autocorrelation indicators (i.e., global and local Moran autocorrelation index and correlation lengths) based on the observed data. The degree of connection between consecutive neighboring sites for each measured variable was also analyzed in order to obtain a quantitative estimation of the nearest neighbors influence to each site in terms of its contribution to the total variability. This allowed attributing the remaining variability to local factors.

In a final step of the analysis, a spatial autoregression model has been used to explore the potential influence of imposed environmental conditions on algal biomass (chlorophyll-*a*), considering the joint contribution of neighbors and local effects (Fischer and Wang, 2011). While neighbors' influence was captured by an autocorrelation term, local effects were embodied in the model by introducing environmental measurements as explanatory independent variables.

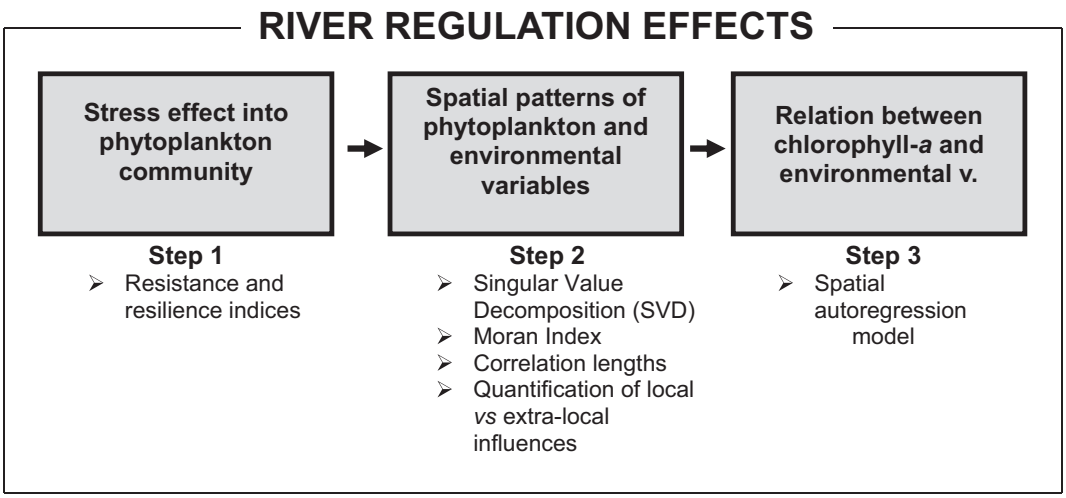

Fig. 2. The methodological workflow.

2.3.1. Quantification of resistance and resilience

We quantified the stress effects of reservoirs into phytoplankton community by defining its resistance and resilience. The calculation of phytoplankton community resistance and resilience were performed comparing values taken upstream (not regulated) and downstream the reservoirs (regulated). In order to better capture the phytoplankton pattern of upstream sites, we used the mean of sites EB04, EB05 and EB06 named as X^{UP}, because of their proximity to the reservoirs. We therefore considered the mean of the upstream sites as the control on which to compare the sites impacted by regulation (Griffiths and Philippot, 2013).

Resistance is an indicator of the capacity of minimal change and was calculated as the difference between the variable measured immediately downstream reservoirs (site EB08) and the corresponding variable measured in upstream sites (X^{UP}).

$$\text{Resistance}\ (\%) = \left(X^{EB08}/X^{UP}\right)\cdot 100 \tag{1}$$

where X stands for the phytoplankton variables measured (biovolume, cell density, chlorophyll-*a* and diversity) at the site indicated by the superscript.

Resilience indicates the ability of phytoplankton to return to initial levels (recovery) after disturbance. Resilience was estimated on the downstream reservoir sites using the following ratio:

$$\text{Resilience}\ (\%) = \left(X^{DOWN}/X^{UP}\right)\cdot 100 \tag{2}$$

DOWN indicates the different sites in downstream section (from EB08 to EB12 sites).

2.3.2. Spatial structure analysis using singular value decomposition (SVD)

The spatial structure of the phytoplankton community and environmental variables was analyzed by means of singular value decomposition (SVD). This is a technique of data dimensionality reduction and may be seen as a generalization of eigenvalue decomposition for rectangular matrices. It consists of a decomposition of rectangular matrix into a product of three matrices which help to interpret the data structure.

Briefly, we constructed a dataset for every measured variable constituted by tables of space × time. These are handled as rectangular matrices M of *m* columns (*m*: number of spatial sites) and *n* rows (*n*: number of campaigns). M matrix can be conveniently factorized in its time and space components using the SVD. Briefly, matrix *M* is factorized as $M = U \cdot \Sigma \cdot V^T$, where *U* is an m × m unitary matrix, Σ is a m × n rectangular diagonal matrix with non-negative real numbers on the diagonal, and V is an n × n real or complex unitary matrix. The diagonal entries σ_i of Σ are known as the singular values of *M*. The columns of U and the columns of V are called the left-singular vectors and right-singular vectors of M, which in our case captured the time and space contributions respectively. Furthermore, U vectors are the eigenvectors of MM^T and V vectors are the eigenvectors of M^TM. The non-zero singular values of M (the diagonal entries of Σ) are the square roots of the non-zero eigenvalues of both M^TM and MM^T.

Contribution c_i of each site *i* to the spatial variability can be calculated using the right singular vectors V, according to the following expression:

$$c_i = \frac{\sum_{j=1}^{n} \sigma_j V_{ij}^2}{\sum_{j=1}^{n} \sigma_j} \tag{3}$$

where v_{ij} is the component *i* of the of the *j* right-singular vector. The sum in the denominator normalizes the weight of the singular values σ_j so that their sum equals unity, and taking into account that V vectors are normalized (i.e., $\sum_{j=1}^{n} V_{ij}^2 = 1$); altogether $\sum_{i=1}^{n} c_i = 1$.

2.3.3. River network analysis

Network analysis was used to explore the structural properties of the set of items (nodes, sites) and the connections between them (links). We characterized each sampling site as the node *i* linked with a neighbor node *j*. Its network structure can be captured by means of the adjacency matrix A, known as spatial-neighborhood matrix, defined as $A_{ij} = 1$ if nodes *i* and *j* are connected, $A_{ij} = 0$ otherwise. Also, we considered that a given node was not affected by itself, so $A_{ii} = 0$. This implies restricting the neighbors' influence to those nodes directly linked to the one considered. In our case, we assumed that the adjacency matrix A associated to the river was not symmetrical since measured variables under concern could only run downstream on the direction of river flow. Thus, the adjacency matrix is assumed to be low-triangular (i.e., a node can be only affected by those located upstream). Therefore, for two connected nodes *i*,*j* $A_{ij} = 1$ if i > j and $A_{ji} = 0$ otherwise. Hence, this implies that the end nodes are considered closed and their measured values taken as boundary conditions (Ginebreda et al., 2018).

2.3.4. Spatial correlation: the Moran index

We explored the continuity and the degree of connection between neighboring sites and identified the influence of neighbors and local factors into the variability of the phytoplankton variables by means of spatial autocorrelation indexes (global and local Moran indexes). We used the Moran index to obtain a first picture of the continuity patterns of the environmental and biological variables of the Ebro. The Moran index (Moran, 1950) is widely used as a measure of spatial autocorrelation in exploratory analyses (Li et al., 2007), and is defined as the two-point correlation for all pairs of consecutively connected sites or lag-1 correlation:

$$Moran\_I = \frac{n\sum_{i=1}^{n}\sum_{j=1}^{n} A_{ij}(x_i-\mu)(x_j-\mu)}{\left(\sum_{i=1}^{n}\sum_{j=1}^{n} A_{ij}\right)\left(\sum_{i=1}^{n}(x_i-\mu)^2\right)} \tag{4}$$

where x_i is the observation of variable *x* at site *i*, μ its mean and *n* the number of monitoring sites (Chen, 2013; Moran, 1950). Since Moran_I calculation requires the use of a symmetric adjacency matrix, here we used $1/2(A^T + A)$ as a symmetrized version of matrix *A*. Furthermore it is row-standardized (i.e., rows sum up to 1) (Li et al., 2007). Moran_I was conveniently calculated following (Chen, 2013). This author showed that Eq. (4) is equivalent to:

$$Moran\_I = \sum_i \sum_j \bar{A}_{ij} z_i z_j = z^T \bar{A} z \tag{5}$$

where $z = (x - \mu) / \sigma$ (*x* standardized) and $\bar{A}$ is a normalized version of *A*, so that $\bar{A}_{ij} = A_{ij} / \sum_{ij} A_{ij}$ and $\sum_{ij} \bar{A}_{ij} = 1$.

The Moran_I indicates the correlation between neighboring spatial observations of a given variable, and so forth it is a measure of spatial association. Spatial autocorrelation among similar neighbor sites results on positive values of Moran_I and conversely, lack of similarity is reflected on negative Moran_I. For the absence of correlation, the expected Moran_I value is given by the expression $-1 / (n - 1)$ (n = number of sites), which is close to zero for high *n* values.

Moran_I can be disaggregated into local node contributions giving way to the so called "Local Indicator of Spatial Association" (LISA) or in short, Local Moran_I (Anselin, 1995):

$$I_i = z_i \sum_j \bar{A}_{ij} z_j \tag{6}$$

$$\text{with} \qquad Moran\_I = \sum_i I_i \tag{7}$$

Moran's local measures assess the spatial autocorrelation associated with one particular area unit (Fischer and Wang, 2011) which is well suited to do an exploratory analysis of the spatial structure of the river.

2.3.5. Correlation lengths

The correlation length ⩗ can be interpreted as the distance threshold, from which a site no longer has influence on the next one (Ginebreda et al., 2018). In order to study how much the spatial correlation between nodes (sites) varies with the separation distance, we calculated Moran_I at higher lags up to 4 (note that at distance 0 Moran_I equals 1). This requires the use of appropriate lower-triangular adjacency matrices $A_{(d)}$ (d = 2, 3, 4) describing the topology at the respective distances. These matrices can be readily obtained multiplying A (actually $A_{(1)}$) by itself the required number of times, i.e., $A_{(2)} = A \cdot A$; $A_{(3)} = A \cdot A \cdot A = A_{(2)} \cdot A$, and so on. The so-called 'correlation length' ⩗ is the distance at which Moran_I = 0, and it was estimated from the linear fit of Moran_I as a function of the topological distance (Dakos et al., 2010) taking it as the intercept with the x-axis. Topological distances can be approximately converted to real distances (in km) multiplying by the mean separation distance (km) between consecutive sites (Ginebreda et al., 2018). This was calculated for phytoplankton and environmental variables.

2.3.6. Quantifying local and neighbor contributions

For a given variable the effect of neighbor sites on each site can be generally described using a simple spatial autoregression model (SAR). This can be simply expressed by means of the spatial autocorrelation Eq. (8) (Fischer and Wang, 2011):

$$x_i = \rho \cdot \sum_{j=1}^{n} A_{ij} \cdot x_j + \varepsilon_i \tag{8}$$

where x_i can be a measured variable at node i and ρ an autocorrelation parameter to be determined. Written in compact matrix form:

$$x = \rho \cdot Ax + \varepsilon \tag{9}$$

where A is the above-mentioned adjacency matrix, x is an n-dimension vector (n = number of nodes) of measurements of the variable considered, ε is an n-dimension vector reflecting the local effects and ρ is a correlation coefficient to be determined. The two terms in Eqs. (8) and (9), capture respectively the neighbors' and local influences. The correlation parameter ρ was calculated by both ordinary least squares (OLS) and maximum likelihood estimation (MLE), being the latter considered the most reliable method (Fischer and Wang, 2011).

The relative contributions of both neighbors and local sources on the variables can be quantified at the river network scale. To do so, Eq. (9) was left multiplied by x^T and both terms were divided by $x^T x$:

$$1 = \rho \cdot \frac{x^T A\, x}{x^T x} + \frac{x^T \varepsilon}{x^T x} \tag{10}$$

The first and second terms respectively provide quantitative estimations of the overall neighbor influence and of the local contributions normalized to unity for the variable under study at the river stretch level (Ginebreda et al., 2018). In the present study Eq. (10) was applied to the phytoplankton and environmental variables.

2.3.7. The spatial autoregression model (SAR model)

We performed a spatial autoregression model (SAR) to take into account neighbor effects and local contributions of environmental variables to algal biomass (chlorophyll-*a*). The SAR model can be generalized by combination with a conventional linear regression multivariate model (Fischer and Wang, 2011), as per equation:

$$x_i = \rho \cdot \sum_{j=1}^{n} A_{ij} x_j + \sum_{q=1}^{m} \beta_q y_{iq} + \varepsilon_i \tag{11}$$

where y_{iq} ($q = 1 \ldots m$) is a vector of independent variables associated to site i, β_q are the corresponding coefficients, and ε_i an error term. Written in compact matrix form, Eq. (11) reads:

$$x = \rho \cdot Ax + y\beta + \varepsilon \tag{12}$$

We analyzed the relationship between chlorophyll-*a* (dependent variable) and nutrients, temperature, conductivity and water flow as independent variables using the above SAR model (Eqs. (11), (12)). Parameters ρ and β_q were determined by regression.

We first developed models for the whole river section and later we explored separate models for upstream and downstream stretches to check for differences between the two. Therefore, separate models were calculated for (a) sites upstream the dams (sites EB01 to EB06); (b) sites downstream the dams (sites EB07 to EB012) and (c) all sites. Best independent variables were selected by step-wise regression.

All calculations were carried out in a spread sheet using Excel (Microsoft®) and graphs were performed using SigmaPlot 13.

3. Results

3.1. Spatial indicators of phytoplankton's response to stress: resistance and resilience

The resistance of chlorophyll-*a* to the reservoirs impact was low (17.3%) while phytoplankton diversity showed a substantially larger resistance (>100%). Biovolume resistance accounted for 32.3% and cell density for 24.8% (Table 1a).

The resilience, that is, the rate of recovery for the phytoplankton variables, was incomplete for biovolume, cell density and chlorophyll-*a*. The maximum recovery with respect the mean of the previous upstream sites (EB04, EB05 and EB06) ranged 19.4–39.1% (Table 1b). The distance needed by biovolume and chlorophyll-*a* to reach the new maximum after the reservoirs impact was at the Ascó site (EB09), while the maximum achieved by cell density was shorter (Flix site, EB08). Contrastingly, diversity completely recovered and even increased slightly after the reservoirs.

3.2. River spatial structure of environmental variables

The spatial pattern of environmental variables (conductivity, temperature, water flow and nutrients) was captured by singular value

Table 1
(a) Resistance and (b) resilience of studied phytoplankton variables.

a

Resistance	%
Biovolume	32.3
Cell density	24.8
Chlorophyll-*a*	17.3
Diversity	113.5

b

Resilience %	Distance 1 (EB08)	Distance 2 (EB09)	Distance 3 (EB10)	Distance 4 (EB11)	Distance 5 (EB12)
Biovolume	32.3	39.1	34.7	21.4	20.1
Cell density	24.8	21.9	23.3	8.6	10.1
Chlorophyll-*a*	17.3	19.4	15.6	14.8	13.5
Diversity	113.5	104.9	108.9	100.1	105.2

decomposition (SVD) analysis of the corresponding data matrices using V vectors (right singular vectors). The first two vectors (Fig. 3a–f) accounted for ca. 80% of the data variability (conductivity 93.1%; temperature 89.1%; water flow 85.8%; SRP 73.4%; DIN 80.9% and DON 70.7%). The analysis indicated that for all these variables the upstream sites were well separated from the downstream sites. The Almatret site (EB07), located in between the dams, was mostly grouped with downstream sites. In all cases, the discrimination was only related to the second singular vector (V2).

The respective site contributions to the variability of environmental variables (Fig. S1) indicates a rather regular variability among all sites. Conductivity, DIN, and DON had a major contribution in the first six

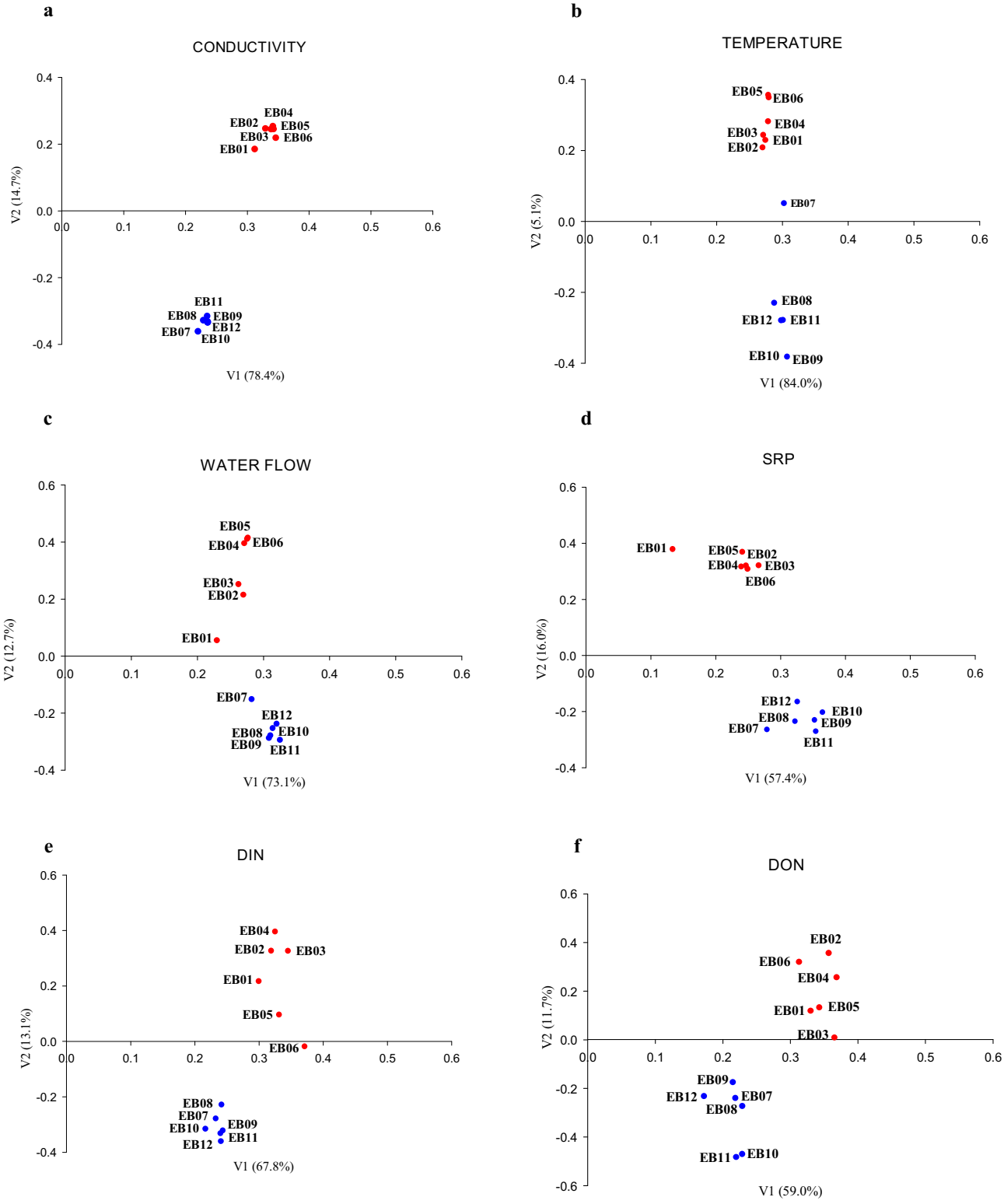

Fig. 3. Representation of the first two Right Singular Vectors (explained variance given in parentheses) for the environmental variables. Upstream sites (EB01 to EB06) are circled in red; downstream sites (EB07 to EB12) are circled in blue. EB01, Zaragoza; EB02, Pina de Ebro; EB03, Quinto; EB04, Zaida; EB05, Sástago; EB06, Escatrón; EB07, Almatret; EB08, Flix; EB09, Ascó; EB10, Móra d'Ebre; EB11, Benifallet; EB12, Xerta.

upstream sites (61.6–62.3%). Temperature, water flow and SRP in the six upstream sites contribution amounted to 44%. In general, for a given river section (upstream or downstream) sites have a similar contribution to the variability of the environmental variables.

3.3. River spatial structure of phytoplankton variables

The spatial pattern of phytoplankton (biovolume, cell density, chlorophyll-*a*, and diversity) captured by the SVD analysis showed that the first two vectors accounted for ca. 70% of the data variability (biovolume 70.6%; cell density 80.1%; chlorophyll-*a* 72.5% and diversity 68.8%, Fig. 4). The upstream sites were separated from the downstream sites for all the considered variables. The Almatret site (EB07), located in between the dams, was grouped with the downstream sites for chlorophyll-*a* and diversity, but close to sites upstream for cell density and biovolume. The first right singular vector (V1) separates upstream and downstream sites for biovolume, cell density, and chlorophyll-*a*, while discrimination in the case of diversity was related to the second singular vector (V2). The first six upstream sites were the main contributors to variability (65.2–80.2%) in biovolume, cell density, and chlorophyll-*a* (Fig. S2). However, diversity variability was evenly divided among all sites (mean per site: 8.3%; upstream and downstream sites had a similar contribution of ca. 50%).

3.4. Longitudinal variations of phytoplankton taxa

In terms of abundance, diatoms dominate the upstream sites while green algae prevailed in the downstream section. Phytoplankton composition of the more abundant taxa (Table 2) upstream of the reservoirs (*Skeletonema potamos*, *Limnothrix planctonica*, *Micractinium pusillum* and large centric diatoms) differed from that downstream of the reservoirs (*Aphanocapsa* sp. and *Oscillatoria* sp.).

3.5. Spatial correlation and connectivity

Spatial autocorrelation (Moran_I) for phytoplankton (biovolume, cell density, chlorophyll-*a* and diversity) and environmental variables (conductivity, temperature, water flow, SRP, DON, and DIN) was calculated taking the variables' mean value for each site averaged from the respective time series. The global Moran_I (Figs. 5a and 6a) indicated a positive spatial autocorrelation for all environmental variables (range: 0.52–0.72, the lowest value corresponding to SRP, and the highest to temperature) as well as for chlorophyll-*a*, biovolume and cell density (range: 0.57–0.73), but negligible correlation for diversity (0.09).

The global Moran_I disaggregated into their local site contributions, that is the local Moran_I, showed a sharp decrease of spatial correlation

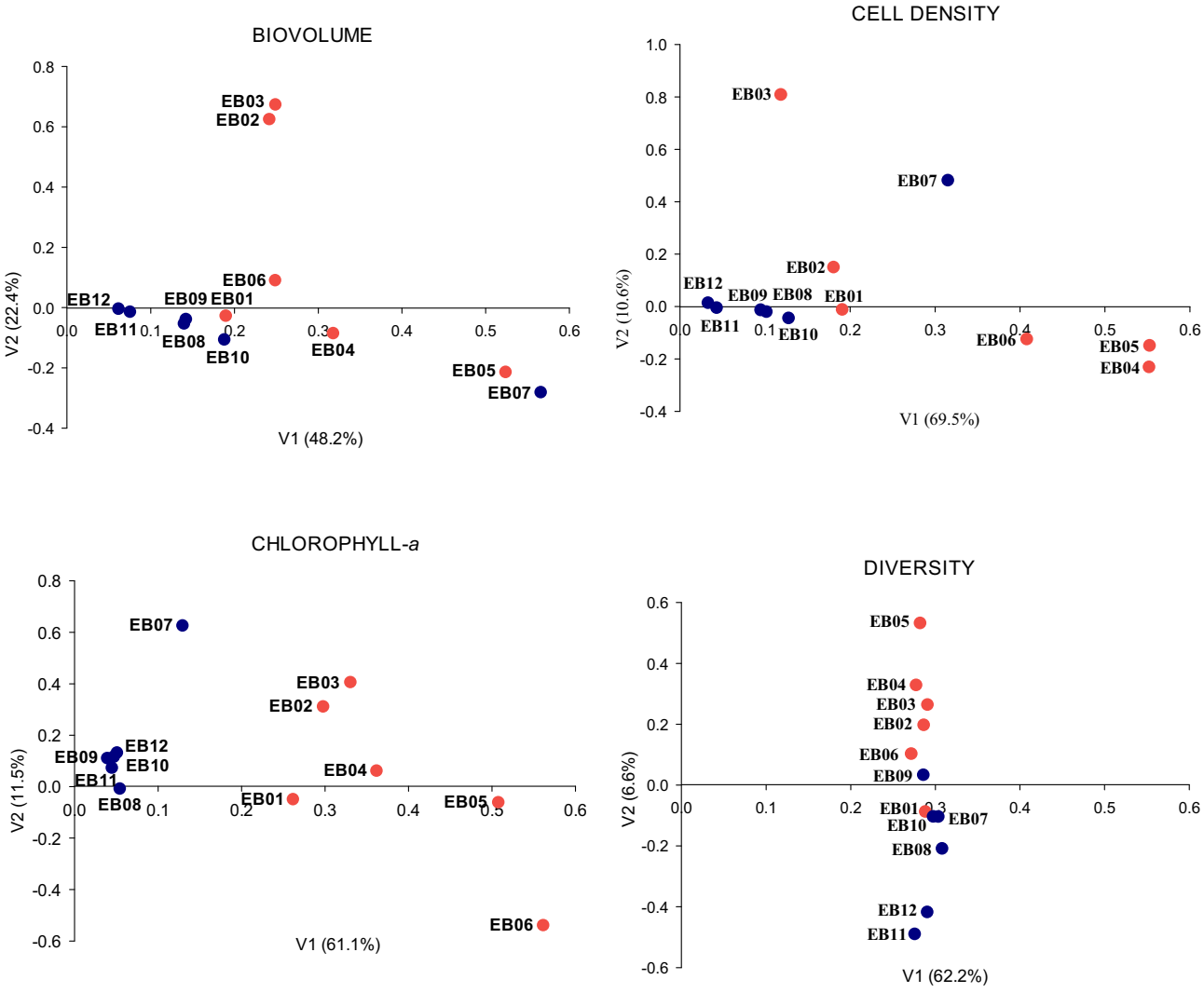

Fig. 4. Representation of the first two Right Singular Vectors (explained variance given in parentheses) for the phytoplankton variables studied. Upstream sites (EB01 to EB06) are circled in red; downstream sites (EB07 to EB12) are circled in blue. EB01, Zaragoza; EB02, Pina de Ebro; EB03, Quinto; EB04, Zaida; EB05, Sástago; EB06, Escatrón; EB07, Almatret; EB08, Flix; EB09, Ascó; EB10, Móra d'Ebre; EB11, Benifallet; EB12, Xerta.

Table 2
The average abundance values (cells/ml) of phytoplankton taxa in the upstream (EB01–EB06) and the downstream (EB07–EB12) sections of all sampling campaigns. The table includes the more abundant taxa from both sections.

Taxa	Upstream	Downstream
Skeletonema potamos	570	4
Large centric diatoms	180	14
Limnothrix planctonica	109	57
Micractinium pusillum	107	5
Planktothrix agardhii	85	36
Small centric diatoms	76	6
Aulacoseira granulata var. *angustissima*	71	6
Actinastrum hantzschii	43	0
Oscillatoria sp.	37	61
Pseudanabaena sp.	31	10
Aphanocapsa sp.	6	123
Cocconeis cf. *placentula*	6	19
Large volvocales	2	17
Planktothrix sp.	2	31
Coelosphaerium sp.	0	29
Pediastrum simplex	0	19

roughly coincident with the dams' occurrence (EB06 and EB07), followed by a progressive recovery downstream (sites EB09–EB12) for both variables (Figs. 5b and 6b). Biovolume shifted from 0.102 to −0.002, cell density from 0.12 to 0.017 and chlorophyll-*a* from 0.085 to −0.017. The Shannon-Wiener diversity showed erratic values along the studied section.

The spatial correlation of conductivity, temperature, water flow, DIN, and DON decreased in Escatrón (EB06) close to 0, indicating lack of similarity between consecutively connected sites (EB05 and EB07). The spatial correlation of conductivity, DIN and DON decreased further in Almatret (EB07) followed by a recovery downstream (Fig. 5b). SRP presented a smooth positive spatial correlation (0.02–0.04) along the upstream sites (EB01 to EB06), and reached a minimum at Almatret (EB07), followed by an increase up to 0.14 from Flix (EB08) to Benifallet (EB11). Sites EB01 and EB12 are considered end nodes (i.e., without external connections) implying that their measured values provide boundary conditions. These results on spatial correlations slightly decreased with respect to their immediate internal neighbors. This situation was observed, for instance, in Xerta (EB12) with respect to Benifallet (EB11) for all the aforementioned environmental variables.

The distance threshold (based on the correlation lengths) at which a site has no influence on the next site downstream was calculated in topological units (TU). Even though monitoring sites are not evenly distributed along the river, one might consider the mean distance between sampling sites (30.5 km) to be roughly equivalent to a topologic distance of 1. Hence, the correlation lengths can be readily transformed into real distances (km) after multiplying by this factor. Correlation lengths of phytoplankton and environmental variables were lower (2.0–4.3 TU) when the whole river section was considered than when river sections were considered separately (2.8–16.5 TU, upstream; 2.4–17.2 TU, downstream), with the only exception of SRP (Table 3, Figs. S3 and S4). The distances of environmental variables were within the range 3.4–17.2 TU, slightly higher than those of phytoplankton variables, 2.0–13.4 TU.

The correlations lengths of environmental variables (except SRP) were about four topologic units (120 km) in the whole river. The correlation length of the two sections (upstream and downstream) showed high values for all variables, being DIN (13.5–17.2 TU) the highest, and SRP (3.1–3.6 TU) the lowest. Conductivity, temperature, and DON presented higher values in the upstream section while water flow, SRP and DIN were higher in the downstream segment (Table 3a and Fig. S1).

Regarding the correlation lengths of phytoplankton variables, biovolume, cell density and chlorophyll-*a* were about three topologic units (90 km), while diversity showed a lower value (60 km) when all river sites were considered. Diversity had lower values (2.8–2.4 TU) and chlorophyll-*a* the highest (up to 8.3 TU) upstream, and increased up to 13.4 TU, downstream. As a matter of fact, the downstream section showed the maximum values, with the exception of diversity (Table 3b and Fig. S2). In all cases, values of r^2 ranged from 0.75 to 0.99.

3.6. Local and neighbor contributions

The respective contributions of neighboring vs. local factors were over 60% in environmental variables. The highest extra-local contribution was for temperature (86%) and water flow (87%), while nutrients (62–79%) and conductivity (70%) had a lower neighbor contribution (Fig. 7a). The neighbor's contribution of phytoplankton variables was ca. 30% for biovolume and diversity, 63.3% for cell density and 55.4% for chlorophyll-*a* (Fig. 7b). The results indicated that phytoplankton variables had greater local contribution than environmental variables.

a

	Global Moran I.
Conductivity	0.69
Temperature	0.72
Water flow	0.60
SRP	0.52
DIN	0.63
DON	0.69

b

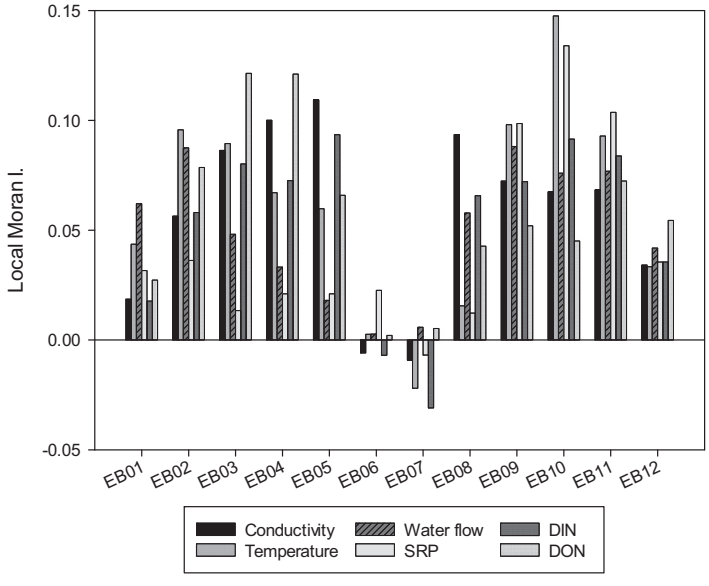

Fig. 5. a) Spatial correlation of environmental variables using Local Moran_I. b) Global Moran Index.

a

	Global Moran I.
Biovolume	0.57
Cell density	0.73
Chlorophyll-a	0.71
Diversity	0.09

b

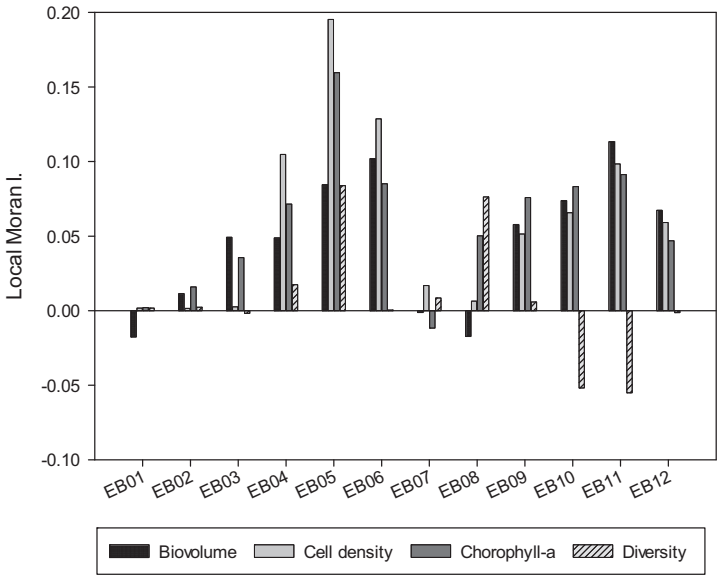

Fig. 6. a) Spatial correlation of phytoplankton variables using Local Moran_I. b) Global Moran Index.

3.7. Algal biomass spatial autoregression model

The longitudinal distribution of algal biomass (chlorophyll-*a*) was analyzed using spatial multilinear regressions together with the most closely related environmental variables (nutrients, temperature, conductivity and water flow). The best models for the whole river section and for the upstream and downstream sections are summarized in Table 4. The obtained correlation coefficients (r^2) were good for the whole river and the upstream section (0.60 and 0.83 respectively) and poor for the downstream section (0.26), but statistically significant in the three cases. The F-value was high for the upstream section (173.34), which gave extra confidence on the r^2 value.

Chlorophyll-*a* appeared positively related with conductivity and negatively correlated with soluble reactive phosphorus (SRP) when the whole river section was considered. When only the upstream section was considered, chlorophyll-*a* appeared negatively related to SRP and water flow. Chlorophyll-*a* in the downstream stretch was negative related to conductivity and DON.

Table 3
Estimation of correlation length (L) expressed in topological units (TU) for (a) environmental variables and (b) phytoplankton variables, considering the whole river and the upstream and downstream sections.

a

	All sites	Upstream	Downstream
Conductivity	3.7	16.5	5.6
Temperature	3.9	15.8	6.9
Water flow	4.3	6.3	9.2
SRP	3.4	3.1	3.6
DIN	3.7	13.5	17.2
DON	4.0	7.6	5.0

b

	All sites	Upstream	Downstream
Biovolume	3.3	3.6	3.7
Cell density	2.8	2.9	4.2
Chlorophyll-*a*	3.3	8.4	13.4
Diversity	2.0	2.8	2.4

The inclusion of the neighbor effects contributed positively to all models improving the correlation between chlorophyll-*a* and environmental variables. So forth, the upstream stretch was more influenced by neighbors (coefficient 0.97) than those in the downstream section (coefficient 0.13).

4. Discussion

Chlorophyll-*a* and its associated biomass variables biovolume and cell density were affected by the reservoirs presence, showing a low resistance as well as a poor recovery downstream. However, diversity even increased downstream of the reservoirs; the substantial loss of biomass contrasted to the increase of species diversity, possibly a result of species replacement by means of some opportunistic algae which took advantage of the new environmental conditions imposed by the reservoirs (Petraitis et al., 1989).

Not only the phytoplankton variables were affected by the reservoirs; also the environmental variables were affected on their spatial variability, which showed a clear separation between the sites located upstream (sites EB01 to EB06) versus those downstream (EB08 to EB12) the reservoirs. The reservoirs, therefore, fragmented the river (Dynesius and Nilsson, 1994) in both the biological and environmental compartments of the river ecosystem. The separate analysis of the different environmental variables reflected the higher contribution to variability patterns in the upstream sites, especially for conductivity and nitrogenous forms (DIN and DON) as well as a more homogenous pattern downstream. The large reservoirs in the Ebro, interrupt the exchange of nutrients between the two river sections (Friedl and Wüest, 2002; von Schiller et al., 2016), which were not so obvious in the water flow and temperature which show more homogeneous patterns in the two river sections. The conductivity and nutrient fluctuations could co-occur with the spatial distribution of the phytoplankton variables, which also showed higher variability pattern in the upstream sites. The hydraulic regulation in the downstream stretch probably was behind the decrease of this conjoint variability. Overall, there was a higher spatial variability in the upstream section, a reflection of the heterogeneous structure of the river, which potentially allowed rapid ecosystem reorganizations and interactions (Petraitis et al., 1989). However, the downstream stretch increased in local homogeneity, as said, mostly reflected in the patterns of biovolume, cell density, and

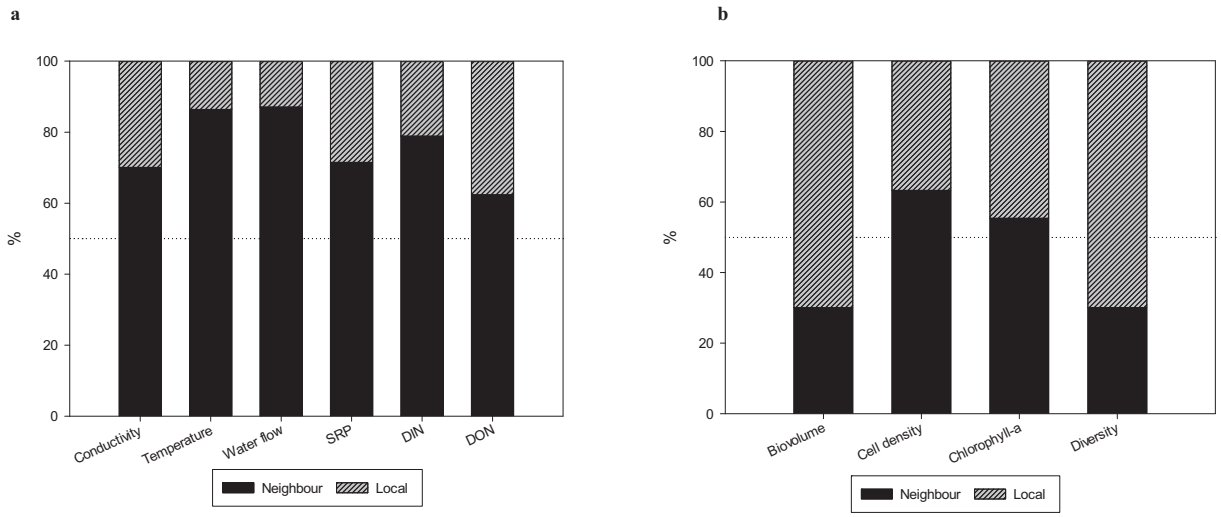

Fig. 7. Local and neighbor contribution using Eq. (10) (autocorrelation parameter ρ estimated by MLE) (a) environmental variables (b) phytoplankton variables.

chlorophyll-*a*, but not in the diversity pattern which was evenly distributed among the sites of the two sections.

The difference between phytoplankton variables associated with biomass (biovolume, cell density, chlorophyll-*a*) with respect to those describing the community structure (diversity) was also highlighted by the spatial analysis. As previously suggested, diversity remains steady because species replacement rather than the decrease in the number of species is the operating mechanism. This follows the adaptive response or autogenic changes of the phytoplankton taxa (Peterson and Stevenson, 1992) to the different environmental conditions occurring in each river section. The phytoplankton community in the Ebro is strongly affected in its composition by the reservoirs (Sabater et al., 2008; Tornes et al., 2014), in a similar way as it occurs in other systems elsewhere (Billen et al., 1994; Istvanovics et al., 2010; Picard and Lair, 2005). On the other hand, the variations in biomass are guided by local factors (i.e. nutrient availability, light, temperature) which determine the growth and success of phytoplankton assemblages (Reynolds, 2006).

The respective site's contribution (Local Moran I) to the spatial variability highlights the existence of an increasing spatial correlation upstream the dams and a decrease in between the reservoirs. The loss in spatial correlation in the environmental and phytoplankton variables in this area can be attributed to the effects that reservoirs produce both on the immediate river upstream site (EB06, Escatrón) as well as in the site placed in between (EB07, Almatret). This pattern confirms the extent that the hydrological river fragmentation shaped the longitudinal structure of environmental conditions and phytoplankton variables.

The topological distance threshold at which a site had no influence on the next downstream was longer for environmental than for phytoplankton variables. This difference highlights the fact that most of the sensitivity of river ecosystems is constrained within the framework of the physical-chemical conditions. This accounts for the increase in connectivity which can be seen when considering separately the upstream and downstream sections emphasizing their functioning as two distinct rivers. The reason for this difference lies in the evidence that the longitudinal dynamics of environmental variables have a strong neighbor influence, stronger than the phytoplankton variables. The longitudinal dynamics of these are more complex and results of a mixture of local and neighbor influences. In particular, cell density and chlorophyll-*a* were more influenced by the contiguous river stretches (or neighbors) than diversity which was seemingly more affected by local factors because of the rapid colonization of opportunist species after the reservoirs.

The application of spatial multivariate auto-regression models to chlorophyll-*a* patterns, allowed separating the contribution of the spatial autocorrelation term as well as the relevance of local environmental variables (nutrients, water flow, temperature, and conductivity) as independent explanatory variables. Both the overall river as well as the separated two river segments showed that neighbors' effect on the chlorophyll-*a* was positive, that is, that values in each river sites were influenced by upstream ones. However, that influence of neighbor sites decreases considerably downstream of the dams, leading to individuality. Planktonic chlorophyll-*a* correlated differently with environmental variables in upstream or downstream sections. The soluble reactive phosphorus (SRP) contributed negatively to the upstream part, meaning that this nutrient was in deficit because of the large growth of phytoplankton and the associated depletion of this nutrient. This is a common situation observed elsewhere (Smith, 1984), which might lead even to the activation of enzymatic extracellular packages to use organic phosphorus (Artigas et al., 2012). Whereas, conductivity and dissolved inorganic nitrogen (DON) were negatively related to the phytoplankton biomass in the downstream section.

Our analysis shows that effects of dams cause river fragmentation in terms of the structure and functioning of environmental characteristics and phytoplankton community. The presence of dams caused a disruption of the spatial autocorrelation as well as a decrease in the natural connectivity. Our study highlighted a clear separation between the river segments upstream and downstream the dams which is reflected

Table 4
Multilinear spatial autoregression models relating the planktonic chlorophyll-*a* (Chl-a) to environmental factors. The number of observations/cases (n), correlation coefficient (r^2), data variability (F) and significance (p-value) are given. A is the adjacency matrix; the product A·Chl-a captures the neighbor effect (Eq. (10)); SRP, soluble reactive phosphorus; Cond, conductivity; DON, Dissolved Organic Nitrogen; WF, water flow.

Relationships	n	r^2	F-value	p-Value
The whole river				
Chl-a = −2.47 + 0.64 A·Chl-a + 0.01 Cond-0.09 SRP	228	0.60	110.18	7.50E−44
Upstream section				
Chl-a = 10.4 + 0.97 A·Chl-a-0.01 WF-0.10 SRP	114	0.83	173.34	1.57E−41
Downstream section				
Chl-a = 8.41 + 0.13 A·Chl-a-0.004 Cond-0.001 DON	114	0.26	13.03	2.42E−07

in the spatial characteristics of phytoplankton and environmental variables. Even though phytoplankton and environmental variables are tightly related, the dynamics of the two is complex and does not follow linear patterns.

Acknowledgments

This study has been financially supported by the EU FP7 project GLOBAQUA [Grant Agreement No. 603629], the NET-Scarce project [Redes de Excelencia CTM2015-69780-REDC] and by the Generalitat de Catalunya [Consolidated Research Groups: 2014 SGR 418—Water and Soil Quality Unit].

Appendix A. Supplementary data

Supplementary data to this article can be found online at https://doi.org/10.1016/j.scitotenv.2018.06.096.

References

Amoros, C., Bornette, G., 2002. Connectivity and biocomplexity in waterbodies of riverine floodplains. Freshw. Biol. 47, 761–776.
Anselin, L., 1995. Local Indicators of Spatial Association—LISA. Geogr. Anal. 27, 93–115.
Artigas, J., Soley, S., Perez-Baliero, M.C., Romani, A.M., Ruiz-Gonzalez, C., Sabater, S., 2012. Phosphorus use by planktonic communities in a large regulated Mediterranean river. Sci. Total Environ. 426, 180–187.
Batalla, R.J., Vericat, D., 2011. An appraisal of the contemporary sediment yield in the Ebro Basin. J. Soils Sediments 11, 1070.
Batalla, R.J., Gómez, C.M., Kondolf, G.M., 2004. Reservoir-induced hydrological changes in the Ebro River basin (NE Spain). J. Hydrol. 290, 117–136.
Billen, G., Garnier, J., Hanset, P., 1994. Modelling phytoplnakton development in whole drainage networks: the RIVSTRAHLER model applied to the Seine River system. Hydrobiologia 289, 119–137.
Buendia, C., Herrero, A., Sabater, S., Batalla, R.J., 2016. An appraisal of the sediment yield in western Mediterranean river basins. Sci. Total Environ. 572, 538–553.
Bunn, S.E., Arthington, A.H., 2002. Basic principles and ecological consequences of altered flow regimes for aquatic biodiversity. Environ. Manag. 30, 492–507.
Chen, Y., 2013. New approaches for calculating Moran's index of spatial autocorrelation. PLoS One 8, e68336.
Dakos, V., van Nes, E.H., Donangelo, R., Fort, H., Scheffer, M., 2010. Spatial correlation as leading indicator of catastrophic shifts. Theor. Ecol. 3, 163–174.
Dale, V.H., 2001. Challenges in the development and use of ecological indicators. Ecol. Indic. 1, 3–10.
Delong, M.D., Thorp, J.H., 2006. Significance of instream autotrophs in trophic dynamics of the Upper Mississippi River. Oecologia 147, 76–85.
Dynesius, M., Nilsson, C., 1994. Fragmentation and flow regulation of river systems in the Northern Third of the World. Science 266, 753–762.
Fischer, M., Wang, J., 2011. Spatial Data Analysis: Models, Methods and Techniques.
Friedl, G., Wüest, A., 2002. Disrupting biogeochemical cycles - consequences of damming. Aquat. Sci. 64, 55–65.
Frissell, C.A., Liss, C.E., Warren, C.E., Hurley, M.D., 1986. A hierarchical framework for stream habitat classification; viewing streams in a watershed context. Environ. Manag. 10, 199–214.
Ginebreda, A., Sabater-Liesa, L., Rico, A., Focks, A., Barceló, D., 2018. Reconciling monitoring and modeling: an appraisal of river monitoring networks based on a spatial autocorrelation approach - emerging pollutants in the Danube River as a case study. Sci. Total Environ. 618, 323–335.
Griffiths, B.S., Philippot, L., 2013. Insights into the resistance and resilience of the soil microbial community. FEMS Microbiol. Rev. 37, 112–129.
Grimm, V., Wissel, C., 1997. Babel, or the ecological stability discussions: an inventory and analysis of terminology and a guide for avoiding confusion. Oecologia 109, 323–334.
Hillebrand, H., Dürselen, C.-D., Kirschtel, D., Pollingher, U., Zohary, T., 1999. BIOVOLUME calculation for pelagic and benthic microalgae. J. Phycol. 35, 403–424.
Holling, C.S., 1973. Resilience and stability of ecological systems. Annu. Rev. Ecol. Syst. 4, 1–23.
Istvanovics, V., Honti, M., Voros, L., Kozma, Z., 2010. Phytoplankton dynamics in relation to connectivity, flow dynamics and resource availability-the case of a large, lowland river, the Hungarian Tisza. Hydrobiologia 637, 121–141.
Lacorte, S., Barceló, D., et al., 2006. Pilot survey of a broad range of priority pollutants in sediment and fish from the Ebro river basin (NE Spain). Environ. Pollut. 140, 471–482.
Li, H., Calder, C.A., Cressie, N., 2007. Beyond Moran's I: testing for spatial dependence based on the spatial autoregressive model. Geogr. Anal. 39, 357–375.
Lobera, G., Muñoz, I., López-Tarazón, J., Vericat, D., Batalla, R., 2017. Effects of flow regulation on river bed dynamics and invertebrate communities in a Mediterranean river. Hydrobiologia 784, 283–304.
López-Moreno, J.I., Beguería, S., García-Ruiz, J.M., 2002. Influence of the Yesa Reservoir on Floods of the Aragón River, Central Spanish Pyrenees. vol. 6.
Moran, P.A.P., 1950. Notes on continuous stochastic phenomena. Biometrika 37, 17–23.
Navarro-Ortega, A., Barceló, D., 2011. Persistent organic pollutants in water, sediments, and biota in the Ebro River Basin. In: Barceló, D., Petrovic, M. (Eds.), The Ebro River Basin. Springer Berlin Heidelberg, Berlin, Heidelberg, pp. 139–166.
Nilsson, C., Reidy, C.A., Dynesius, M., Revenga, C., 2005. Fragmentation and flow regulation of the world's large river systems. Science 308, 405–408.
Nordstrom, M.C., Bonsdorff, E., 2017. Organic enrichment simplifies marine benthic food web structure. Limnol. Oceanogr. 62, 2179–2188.
Peterson, C.G., Stevenson, R.J., 1992. Resistance and resilience of lotic algal communities: importance of disturbance timing and current. Ecology 73 (4), 1445–1461.
Petraitis, P.S., Latham, R.E., Niesenbaum, R.A., 1989. The maintenance of species-diversity by disturbance. Q. Rev. Biol. 64, 393–418.
Picard, V., Lair, N., 2005. Spatio-temporal investigations on the planktonic organisms of the Middle Loire (France), during the low water period: biodiversity and community dynamics. Hydrobiologia 551, 69–86.
Pimm, S.L., 1984. The complexity and stability of ecosystems. Nature 307, 321–326.
Prats, J., Val, R., Armengol, J., Dolz, J., 2010. Temporal variability in the thermal regime of the lower Ebro River (Spain) and alteration due to anthropogenic factors. J. Hydrol. 387, 105–118.
Reynolds, C.S., 2006. Ecology of Phytoplankton. vol. 1. Cambridge Univ. Press, Cambridge.
Romaní, A.M., Sabater, S., Muñoz, I., 2011. The physical framework and historic human influences in the Ebro River. In: Barceló, D., Petrovic, M. (Eds.), The Ebro River Basin. Springer Berlin Heidelberg, Berlin, Heidelberg, pp. 1–20.
Sabater, S., Artigas, J., Duran, C., Pardos, M., Romani, A.M., Tornes, E., et al., 2008. Longitudinal development of chlorophyll and phytoplankton assemblages in a regulated large river (the Ebro River). Sci. Total Environ. 404, 196–206.
Smith, S.V., 1984. Phosphorus versus nitrogen limitation in the marine-environment. Limnol. Oceanogr. 29, 1149–1160.
Tockner, K., Pennetzdorfer, D., Reiner, N., Schiemer, F., Ward, J.V., 1999. Hydrological connectivity, and the exchange of organic matter and nutrients in a dynamic river-floodplain system (Danube, Austria). Freshw. Biol. 41, 521–535.
Tornes, E., Perez, M.C., Duran, C., Sabater, S., 2014. Reservoirs override seasonal variability of phytoplankton communities in a regulated Mediterranean river. Sci. Total Environ. 475, 225–233.
Vannote, R.L., Minshall, G.W., Cummins, K., Sedell, J.R., Cushing, C.E., 1980. The River Continuum Concept. vol. 37.
von Schiller, D., Aristi, I., Ponsati, L., Arroita, M., Acuña, V., Elosegi, A., et al., 2016. Regulation causes nitrogen cycling discontinuities in Mediterranean rivers. Sci. Total Environ. 540, 168–177.
Wallach, A.D., Dekker, A.H., Lurgi, M., Montoya, J.M., Fordham, D.A., Ritchie, E.G., 2017. Trophic cascades in 3D: network analysis reveals how apex predators structure ecosystems. Methods Ecol. Evol. 8, 135–142.
Ward, J.V., Stanford, J.A., 1983. The serial discontinuity concept of lotic ecosystems. In: Fontaine, T.D., Bartell, S.M. (Eds.), Dynamics of Lotic Ecosystems, pp. 29–42 Ann Arbor Scientific Publishers.
Ward, J.V., Stanford, J.A., 1995. Ecological connectivity in alluvial river ecosystems and its disruption by flow regulation. Regul. Rivers Res. Manag. 11, 105–119.
Wehr, J.D., Descy, J.P., Oct 1998. Use of phytoplankton in large river management. J. Phycol. 34, 741–749.